

Facile Synthesis, Formation Mechanism and Optical Properties of ZnO Nanostructures

Linu M. Johny, N.S. Nirmala Jothi and P. Sagayaraj

Abstract ZnO is a very promising material because of its wide range of applications in electronics, photonics, optics and as energy storage materials. Zinc oxide nanorods were synthesized using a simple hydrothermal method at lower temperature and nano spheres by solvothermal method. The formation process of ZnO nanorods and nanospheres is discussed. The X-ray diffraction pattern indicates that the nanorods and nanospheres have hexagonal wurtzite structure. The high resolution transmission electron microscopy (HRTEM) images reveal that the synthesized ZnO nanorods grow along $\langle 001 \rangle$ direction. The optical properties were studied by UV visible absorption and photoluminescence spectroscopy.

1 Introduction

Nanomaterials of transparent conducting oxides with unique morphologies are currently of great interest to researchers because of wide possibilities in different technological applications. ZnO is a wide band gap (3.37 eV) transition metal oxide n-type semiconductor with large exciton binding energy (60 meV) and has wide range of applications because of its optical, electrical, magnetic, piezoelectric properties [1–3]. It is used in fabricating devices like gas sensors, solar cells and lithium ion batteries [4–6] etc. ZnO nanostructures with different morphologies like nanorods, nanotubes, nanowires, nanosheets, nanobelts, nanoflowers, hierarchial nanostructures [7–12] have been synthesized by various physical methods and wet chemical methods. The synthesis of 1D ZnO have been reported by different physical methods like chemical vapour deposition (CVD), pulsed laser deposition (PLD), MOVCD, template assisted growth [13, 14] and also by wet chemical methods like hydrothermal/solvothermal method, sol-gel method [7, 15, 16]. The

L.M. Johny · N.S. Nirmala Jothi (✉) · P. Sagayaraj
Department of Physics, Loyola College, Chennai, India
e-mail: jmjnirmala@yahoo.co.in

synthesis by wet chemical method is comparatively easy at relatively low temperature. 1D nanostructures with dissimilar surfaces will differ in their geometric and electronic structures and therefore show different functional properties. Therefore, for fabricating devices, it is necessary to control the crystal morphology, size and shape of the faces of metal oxide crystal. Thus one dimensional nanostructures can be used to fabricate various nano devices like UV detectors, nano lasers, solar cells, gas sensors and as anode materials for lithium ion batteries [4–6, 17–19]. Here we report the synthesis and characterization of ZnO nanorods by hydrothermal method at low temperature and nanospheres with hexagonal faces by a simple solvothermal method. The crystalline nature of the sample was characterized using XRD, the morphology of the sample was examined using HRTEM, the band gap was determined by UV-Vis absorption and reflectance spectra, optical properties were studied using room temperature photoluminescence.

2 Experimental

2.1 *Synthesis of ZnO Nanorods*

All chemicals used were of analytical grade and were used without any further purification. 100 ml of 0.1 M ammonia solution and 50 ml of 0.1 M zinc acetate dihydrate solution was prepared. Ammonia solution was taken in a burette and slowly added drop wise into 50 ml zinc acetate solution under mild stirring. A white gelatinous precipitate is formed. It was then stirred for about an hour. The precipitate was thoroughly washed with water several times. The washed precipitate was ultrasonically dispersed in 80 ml of deionized water. It was then transferred to a Teflon lined stainless steel autoclave and kept in a furnace at 100 °C for 12 h. The precipitate was then washed, filtered and dried in vacuum at 80 °C for further characterization.

2.2 *Synthesis of ZnO Nanospheres*

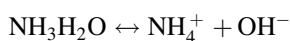
All chemicals used were of analytical grade and were used without any further purification. 1 mmol of zinc acetate dihydrate was dissolved in 160 ml of 1-propanol. It was magnetically stirred for an hour and transferred into a 200 ml Teflon lined autoclave and heated at 160 °C for 24 h. A white precipitate formed was washed with water and ethanol several times and dried at 80 °C for 12 h. It was then calcined at 500 °C for 2 h.

3 Formation and Growth Mechanism

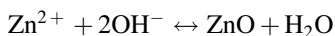
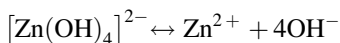
3.1 ZnO Nanorods

ZnO is a polar crystal with Zn rich positive plane $\langle 001 \rangle$ and an oxygen rich negative plane $\langle 00\bar{1} \rangle$. Since we have not used any templates or surfactants for the growth of ZnO nanorods, the concentration of Zn^{2+} to OH^- ions in the solution plays a major role in the morphology of the crystal structure. The ratio of $\text{NH}_4\text{OH}:\text{Zn}(\text{CH}_3\text{COO})_2 \cdot 2\text{H}_2\text{O}$ is 2:1, the OH^- ions are not just a source of hydroxyl ions, but will also act as a capping agent. Due to the high concentration of OH^- ions, they will be adsorbed on the $\langle 001 \rangle$ plane of ZnO. Thus OH^- ions will allow the growth of crystal along $\langle 001 \rangle$ direction [20]. The overall reaction for the growth of ZnO rods may be summarized as follows

Reaction of $\text{Zn}(\text{CH}_3\text{COO})_2 \cdot \text{H}_2\text{O}$ with NH_4OH



Hydrothermal treatment of $\text{Zn}(\text{OH})_2$

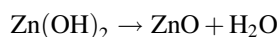
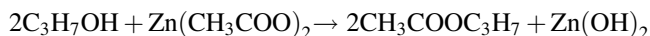


It is concluded that the concentration of OH^- ions in the solution and $[\text{Zn}(\text{OH})_4]^{2-}$ radical plays an important role during hydrothermal process for the formation of ZnO rods.

3.2 ZnO Nanospheres

The formation of ZnO nanospheres is facilitated by the hydrolysis of caboxylate (zinc acetate) and by the condensation reaction in the alcohol medium. The hydroxyl group that binds to the Zn species is released by esterification. Susequently a Zn–O–Zn bond is generated by the condensation of Zn hydroxyl species with elimination of water.

Reaction of $\text{Zn}(\text{CH}_3\text{COO})_2 \cdot 2\text{H}_2\text{O}$ with $\text{C}_3\text{H}_7\text{O}$



4 Characterization

XRD studies to analyze the crystalline nature was made using X PAN analytical X'pert PRO diffractometer with $\text{Cu-K}\alpha$ $\lambda = 1.54060 \text{ \AA}$. The optical absorption spectra of ZnO nanoparticles were characterized by UV-Vis spectrophotometer Shimadzu UV-3600. The High Resolution Transmission Electron Microscopy (HRTEM) and selected area diffraction pattern (SAED) were obtained on a Jeol/JEM 2100 operated at a voltage of 200 kV. Room temperature PL was recorded on a Cary Eclip spectrophotometer with an excitation wavelength of 255 nm.

5 Results and Discussion

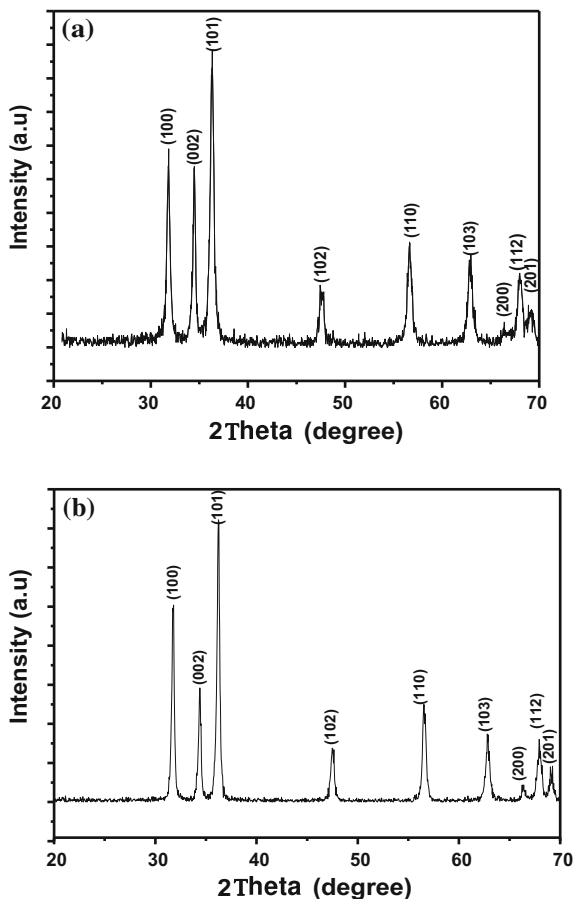
5.1 XRD Analysis

The XRD pattern of the zinc oxide nanorods is given in Fig. 1a and that of nanospheres is given in Fig. 1b. The peaks present in the spectrum confirms the polycrystalline nature of the nanostructures, corresponding to that of hexagonal ZnO with lattice constants $a = 3.249 \text{ \AA}$ and $c = 5.206 \text{ \AA}$. The peak positions matched well with the standard data for ZnO (JCPDS card no. 36-1451). No other crystalline by products are found in the pattern, indicating that the as prepared ZnO has a pure wurtzite nature. The average crystallite size D was calculated using Scherrer equation $D = 0.9\lambda/\beta\cos\theta$. The average crystallite size is about 26 nm and that of nanospheres is 18 nm.

5.2 Williamson-Hall Analysis

In X-ray diffraction, the peak broadening is caused mainly by particle size and lattice strain. Average particle size is usually measured using X-ray profile analysis. It is also seen that crystal imperfections, like lattice dislocations lead to lattice strain and is a measure of lattice constants. To estimate the crystallite size and lattice

Fig. 1 XRD spectra of ZnO
a nanorods, and
b nanospheres



strain the W-H analysis of XRD data was used. In nanocrystalline ZnO the strain induced by crystal imperfections and distortion is calculated by using the formula:

$$\varepsilon = \frac{\beta_{hkl}}{\tan \theta} \quad (1)$$

where ε is the strain, β_{hkl} is the FWHM of the diffraction peak and θ is the Bragg angle. Though the particle size and strain result in peak broadening, they are independent of each other and therefore the peak can be written as sum of particle size and strain as follows:

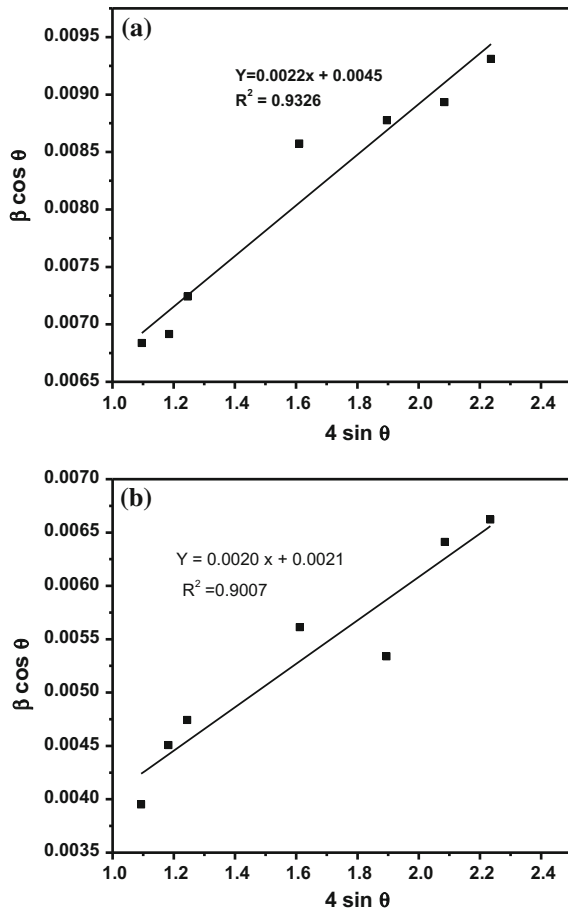
$$\beta_{hkl} = \frac{k\lambda}{D \cos \theta} + 4\varepsilon \tan \theta \quad (2)$$

From the above two equations, we get

$$\beta_{hkl} \cos \theta = \frac{k\lambda}{D} + 4\varepsilon \sin \theta \tag{3}$$

Equations (2) and (3) are known as W-H equations. A W-H plot for the nanostructures is obtained with $4\sin\theta$ along the x-axis and $\beta \cos\theta$ along the y-axis as shown in Fig. 2a, b. The crystallite size of ZnO nanospheres from the plot is around 20 nm which is in good agreement with that calculated using Scherrer formula, but for ZnO nanorods it is found to be 45 nm. The particle size for nanorods does not match with that calculated using Scherrer formula because of the morphology and oriented growth of the crystal in a particular direction. As crystallite size measures the size of the coherent diffracting domains, the crystallite size may not be generally the same as the particle size due to the formation of

Fig. 2 Williamson Hall plot for ZnO **a** nanorods, and **b** nanospheres



polycrystalline aggregates. The micro strain due to the lattice deformation for ZnO nanorods is found to be 0.22 % and that for ZnO nanospheres is 0.20 %.

5.3 High Resolution Transmission Electron Microscopy (HRTEM)

Figure 3a, b gives the HRTEM micrographs of synthesized ZnO nanorods. The samples show almost uniform nanorods with around 25 nm diameter and 150 nm length with an aspect ratio of 6 without much agglomeration. As we can see small bright spots making up the rings, each spot arising from Bragg reflection of an individual crystallite, it is concluded that the ZnO samples have polyananocrystalline

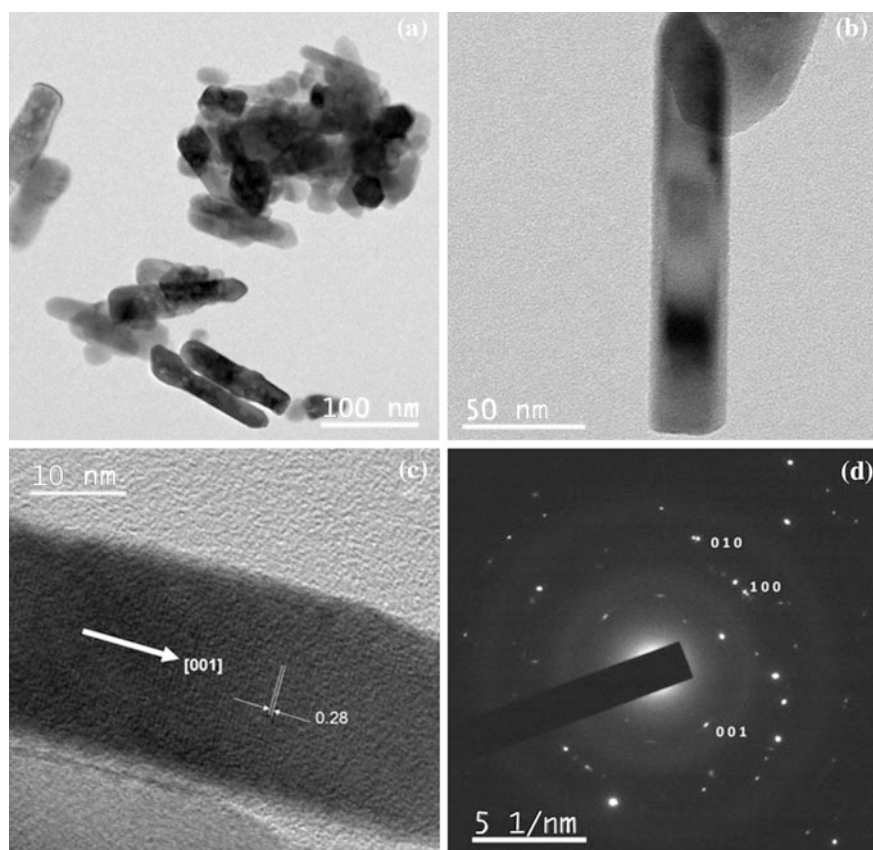


Fig. 3 HRTEM images of ZnO **a** nanorods, **b** single nanorod, **c** Lattice resolved image of single nanorod, and **d** SAED pattern

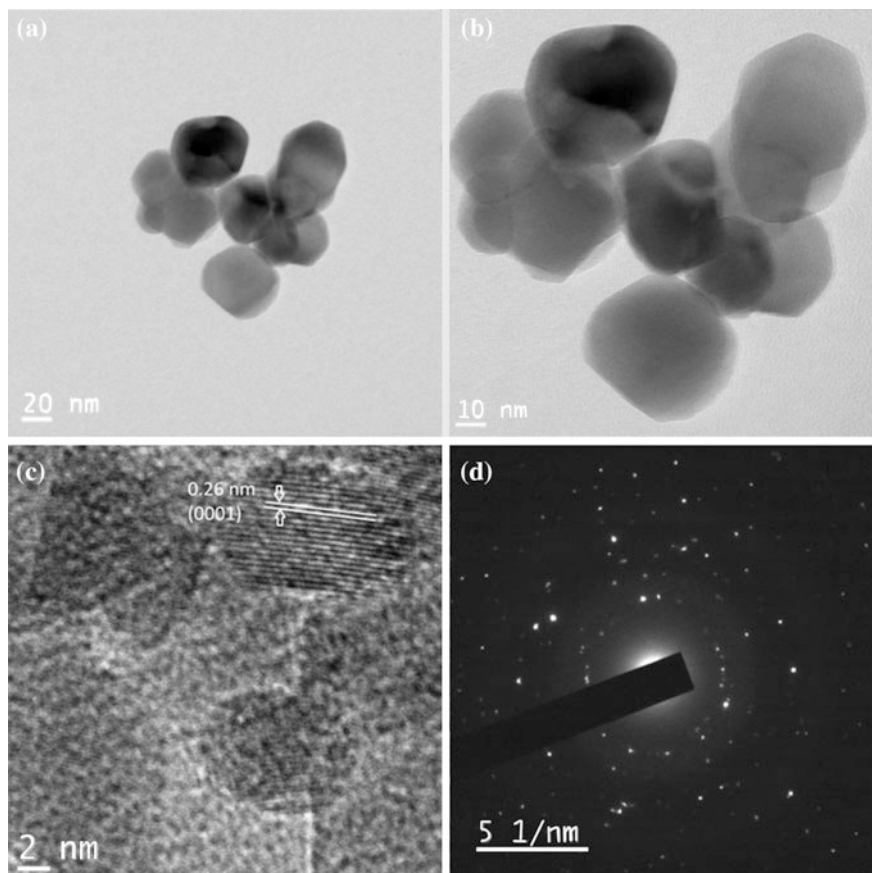


Fig. 4 HRTEM images of ZnO **a** nanospheres, **b** nanospheres with hexagonal faces, **c** Lattice resolved image of single nanosphere, and **d** SAED pattern

nature. Figure 3c shows the image of a single nanorod grown along the $\langle 001 \rangle$ direction. The fringe width of 0.28 nm corresponds to the $\langle 010 \rangle$ plane of ZnO.

Figure 4a, b gives the HRTEM micrographs of synthesized ZnO nanospheres. The samples show almost uniform spheres with around 20 nm diameter without much agglomeration. The hexagonal faces of the spheres can be clearly seen in TEM images. Figure 4c shows the hexagonal face of a single nanosphere. As we can see small bright spots making up the rings, each spot arising from Bragg reflection of an individual crystallite, it is concluded that the ZnO nanostructures have polynanocrystalline nature (Figs. 3d, 4d).

5.4 UV-Vis Spectroscopy

UV-Vis spectroscopy was used to characterize the optical absorptions of ZnO nanoparticles. Figure 5a, b shows the absorption peak of UV spectra of nanorods and nanospheres are at 312 and 340 nm respectively. To determine the optical band gap of the synthesized ZnO the reflectance spectra was carried out. The diffuse reflectance (DR) spectrum for ZnO nanorods, and nanospheres with their corresponding Tauc's plot is shown in Figs. 6a, b and 7a, b. To determine the exact band gap value of ZnO, the reflectance values were converted to absorbance by applying Kubelka-Munk function [21]. The band gap can be determined by the following formula.

Fig. 5 UV-Vis absorption spectrum of ZnO **a** nanorods, and **b** nanospheres

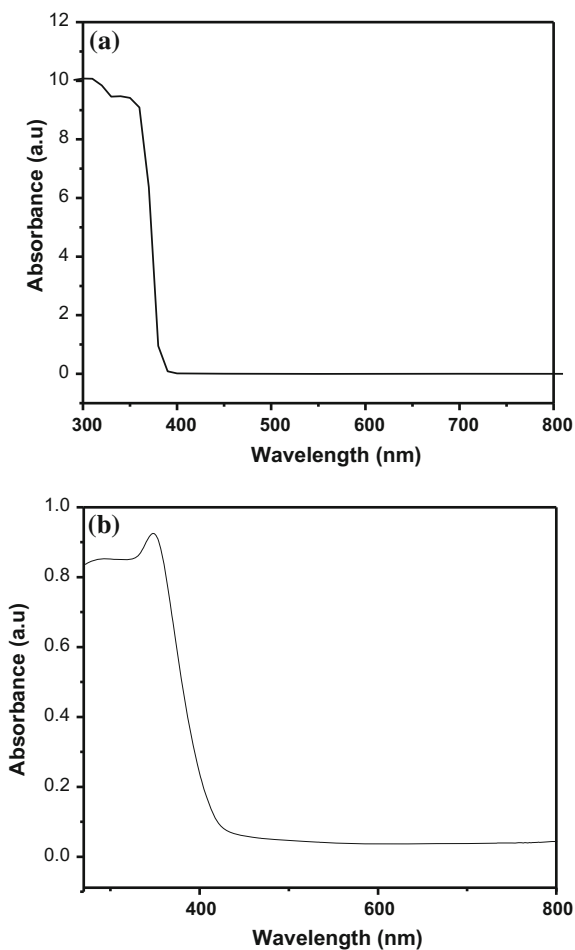


Fig. 6 **a** DR spectrum, **b** Tauc's plot for ZnO nanorods

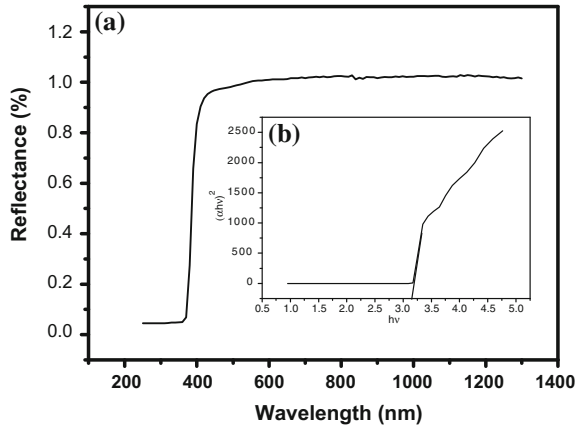
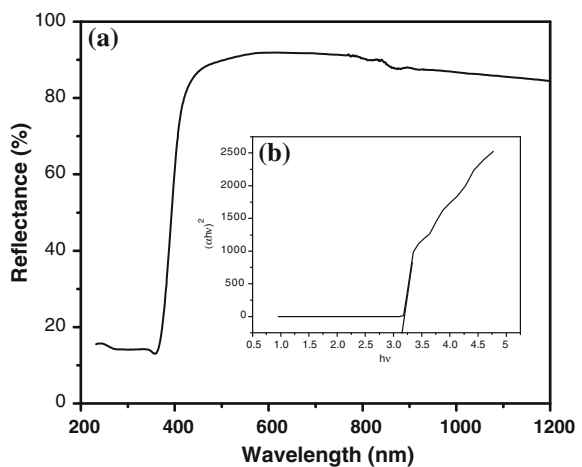


Fig. 7 **a** DR spectrum, **b** Tauc's plot for ZnO nanospheres



$$a = \frac{K(h\nu - E_g)^{n-2}}{h\nu}$$

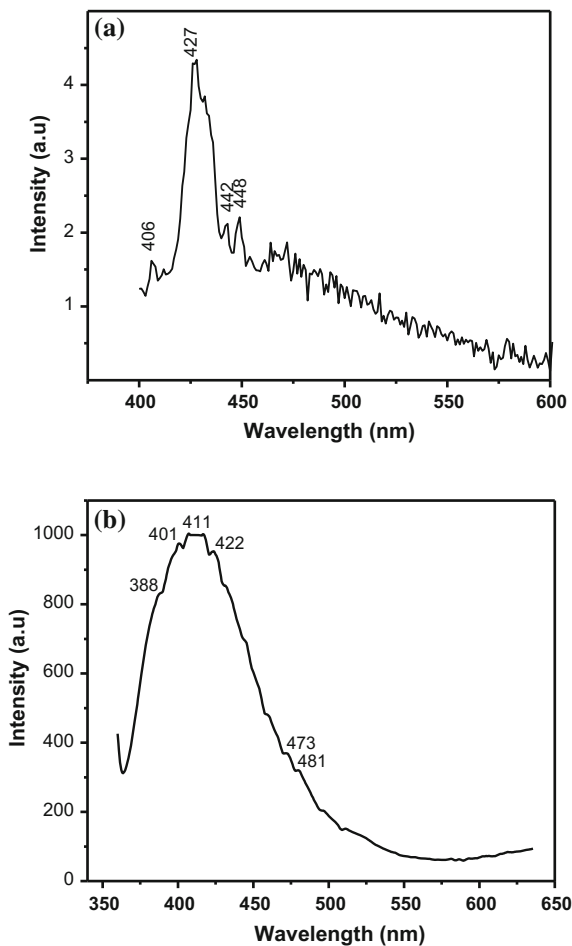
where α is the absorption coefficient, K is a constant, E_g is the band gap, and $n = 1$ for direct transition. The relationship between the absorption co-efficient α and the photon energy $h\nu$ for direct allowed transition is given as $(\alpha h\nu)^2 = B(h\nu - E_g)$ where $h\nu$ is the photon energy E_g is the apparent optical band gap. The direct band gap of $(\alpha h\nu)^2$ against $h\nu$ plot is extrapolated to intersect the energy axis at $\alpha = 0$. The band gap is found to be 3.34 eV for nano rods and 3.39 eV for nano spheres respectively.

5.5 Photoluminescence Studies

Figure 8a shows the photoluminescence spectra of ZnO nanorods. The emission spectra was obtained at an excitation wavelength of 255 nm using a Xe flash lamp. The spectra shows emission only in the blue region with a strong emission peak centered at 428 nm and two peaks at 405 and 448 nm respectively and the well known green luminescence of ZnO at 510 + 50 nm is quenched. Photoluminescence (PL) is an effective tool to study the optical properties and also about the defect levels in semiconductor materials. The origin of luminescence centers are investigated as it finds application in the field of optoelectronics. Luminescence of ZnO in different regions of the visible spectrum (UV-Blue, Green, Yellow) can be due to intrinsic or extrinsic point defects. The deep level emission in ZnO has been attributed to different intrinsic defects in the crystal of ZnO such as oxygen vacancies (V_O), oxygen interstitial (O_i), zinc vacancies (V_{Zn}), zinc interstitial (Zn_i) and oxygen anti-site (O_{Zn}) and zinc anti-site (Zn_O) [22]. Previous PL studies on ZnO nano structures show that the optical properties of ZnO change with crystal morphology even in the absence of dopants [23]. It has been reported that the optical properties ZnO rods are enhanced with increase in their aspect ratio. Zeng et al. [24] reported that blue emission of ZnO nano particles originate from transitions involving Zn interstitial defect states. It is also reported that low temperature annealing provides enough ionization energy and increases the concentration of charge in Zn interstitials, strengthening blue emissions. Monticone et al. [25] also have reported that for ZnO prepared at high OH^- ion concentration the emission in the green region is strongly suppressed. It can therefore be concluded that the strong blue emissions are due to the transition from the Zn interstitial defect states because of the morphology and as the sample is synthesized at low temperatures.

Figure 8b shows the PL spectra of ZnO nanospheres. The emission spectra was obtained at an excitation wavelength of 340 nm using a Xe flash lamp. The spectra shows emission only in the UV region at 388 nm and blue region with a strong emission peak centered at 415 nm and two shoulders are at 401 and 423 nm respectively and the well known green luminescence of ZnO at 510 + 50 nm is quenched. Two minor peaks are seen at 473 and 481 nm respectively. The peak at 388 nm is considered as the characteristic band edge emission of ZnO or the excitonic recombination [23, 25]. Blue emission in ZnO is due to the transition from the Zn interstitial defect states Zn_{ni} slightly below the conduction band to the valence band. Blue emissions can also be due to the extended Zn_{ni} states which are slightly below the simple Zn_{ni} state to the valence band [23]. The many peaks in the blue region can be attributed to emissions from the extended Zn_{ni} to the valence band. Zeng et al. have also done an interesting observation that for blue emissions the excitation wavelength is not in accordance with the band gap, it takes either a slightly higher or lower value. Here the excitation given for ZnO nanorods is

Fig. 8 PL spectrum of ZnO
a nanorods, and
b nanospheres



slightly below the band gap and for ZnO nanospheres it is near band gap value. Therefore it can be concluded that the blue emissions from the nano ZnO spheres is due to the transitions from the several extended sub states related to the Z_{ni} defect states below the conduction band edge.

6 Conclusion

ZnO nanorods are synthesized by a hydrothermal technique at low temperature and ZnO nanospheres are synthesized by solvothermal method. The structural, morphological and optical properties were analyzed. XRD showed that the synthesized ZnO nanorods and nano spheres have hexagonal wurtzite structures. UV-Vis

spectroscopy confirmed the band gap of ZnO nanorods to be 3.34 eV and nanospheres to be 3.39 eV. The PL spectra of ZnO rods was found to be dominated by a strong and sharp emission in the blue region and the exciton emission in the UV region and well known emission in the green region was suppressed. The PL spectra of ZnO nanospheres found to be dominated by a strong and sharp emission in the blue region and the exciton emission in the UV region but the well known emission in the green region was suppressed. 1D ZnO nanostructures are considered ideal as it finds applications in devices like gas sensors, Li ion batteries etc. The blue luminescence of ZnO nanorods and nanospheres would have potential in visible light emission and biological fluorescence labeling application. It can also be used to fabricate UV detectors and solar cells.

References

1. Grundmann, M., Wenckstern, H.V., Pickenhain, R., Nobis, Th, Rahm, A., Lorenz, M.: Electrical properties of ZnO thin films and optical properties of ZnO-based nanostructures. *Superlattices Microstruct.* **38**, 317–328 (2005)
2. Xu, Q., Zhou, S., Schmidt, H.: Magnetic properties of ZnO nanopowders. *J. Alloys Compd.* **487**, 665–667 (2009)
3. Hsu, C.L., Chen, K.C.: Improving piezoelectric nanogenerator comprises ZnO nanowires by bending the flexible PET substrate at low vibration frequency. *J. Phys. Chem. C* **116**(16), 9351–9355 (2012)
4. Wang, X., Li, W., Liu, J., Wang, F., Kong, J., Qiu, S., Cuizhu, H., Lua, L.: Synthesis of nestlike ZnO hierarchically porous structures and analysis of their gas sensing properties. *ACS Appl. Mater. Interfaces* **4**, 817–825 (2012)
5. Barpuzary, D., Banik, A., Panda, A.N., Qureshi, M.: Mimicking heteroleptic dyes for an efficient 1D-ZnO based dye-sensitized solar cell using the homoleptic ruthenium(II) dipyrrophenazine complex as a photosensitizer. *J. Phys. Chem. C* **119**(8), 3892–3902 (2015)
6. Shen, X., Mu, D., Chen, S., Wu, B., Wu, F.: Enhanced electrochemical performance of ZnO-loaded/porous carbon composite as anode materials for lithium ion batteries. *Appl. Mater. Interfaces* **5**, 3118–3125 (2013)
7. Liu, B., Zeng, H.C.: Hydrothermal synthesis of ZnO nanorods in the diameter regime of 50 nm. *J. Am. Chem. Soc.* **125**(15), 4430–4431 (2003)
8. Xu, C., Shin, P., Cao, L., Gao, D.: Preferential growth of long ZnO nanowire array and its application in dye-sensitized solar cells. *J. Phys. Chem. C* **114**(1), 125–129 (2010)
9. Wang, C., Mao, B., Kang, Z., Tian, C.: Solution synthesis of ZnO nanotubes via a template-free hydrothermal route. *Solid State Commun.* **141**(11), 620–623 (2007)
10. Wang, X.D., Song, V.Z., Wang, L.: Nanowire and nanobelt arrays of zinc oxide from synthesis to properties and the novel devices. *J. Mater. Chem.* **17**(8), 711–720 (2007)
11. Su, Y., Li, J., Luo, Z., Lua, B., Li, P.: Microstructure, growth process and enhanced photocatalytic activity of flower-like ZnO particles *RSC Adv.* (2016)
12. Zhang, Y., Xu, J., Xiang, Q., Li, H., Pan, Q., Xu, P.: Brush-like hierarchical ZnO nanostructures: synthesis, photoluminescence and gas sensor properties. *J. Phys. Chem. C* **113**, 3430–3435 (2009)
13. Lu, L., Chen, J., Li L., Wang, W.: Direct synthesis of vertically aligned ZnO nanowires on FTO substrates using a CVD method and the improvement of photovoltaic performance . *Nanoscale Res Lett.* **7**(1), 293 (2012)

14. Wang, X., Ding, Y., Yuan, D., Hong, J., Liu, Y., Wong, C.P., Hu, C., Wang, Z.L.: Reshaping the tips of ZnO nanowires by pulsed laser irradiation. *Nano Res.* **5**(6) (2012)
15. Vassieres, L., Keis, K., Lindquist, S.E.: Purpose built anisotropic metal oxide materials: 3D highly oriented arrays of ZnO. *J. Phys. Chem. B* **105**(17), 3350–3352 (2001)
16. Hung, C.H., Whang, W.T.: A novel low-temperature growth and characterization of single crystal ZnO nanorods. *Mater. Chem. Phys.* **82**(3), 705–710 (2003)
17. Yu, H.C., Bo, T.C., Chih, K.C., Ying, Y., Chun, T.Y., Heng, L., Tzy, R.L., Chien, C.L., Hao, C.K., Shing, C.W., Tien, C.L.: Ultrastrong mode confinement in ZnO surface plasmon nanolasers. *ACS Nano* **9**(4), 3978–3983
18. Alenezi, M.R., Alshammari, A.S., Alzanki, T.H., Jarowski, P., Henley, S.J., Ravi, S., Silva, P.: ZnO nanodisk based UV detectors with printed electrodes. *Langmuir* **30**(13), 3913–3921 (2014)
19. Li, F., Gong, F., Xiao, Y., Zhang, A., Zhao, J., Fang, S., Jia, D.: ZnO twin-spheres exposed in (001) facets: stepwise self-assembly growth and anisotropic blue emission. *Acsnano* **7**(12), 10482–10491 (2013)
20. Alenezi, M.R., Henley, S.J., Emerson, N.G., Ravi, S., Silva, P.: From 1D and 2D ZnO nanostructures to 3D hierarchical structures with enhanced gas sensing properties
21. Baraneedharan, P., Siva, C., Nehru, K., Sivakumar, M.: Investigations on structural, optical and electrochemical properties of blue luminescence SnO₂ nanoparticles. *J. Mater. Sci.: Mater. Electron.* **25**, 255–261 (2014)
22. Naveed ul, H.A.: Linköping studies in science and technology. Dissertation No. 1378 luminescence properties of ZnO nanostructures and their implementation as white light emitting diodes (LEDs) by ISBN: 978-91-7393-139-7
23. Zeng, H., Duan, G., Li, Y., Yang, S., Xu, X., Cai, W.: Blue luminescence of ZnO nanoparticles based on non-equilibrium processes: defect origins and emission controls. *Adv. Funct. Mater.* **20**, 561–572 (2010)
24. Cao, B., Teng, X., Heo, S.H., Li, Y., Cho, S.O., Li, G., Cai, W.: Different ZnO nanostructures fabricated by a seed-layer assisted electrochemical route and their photoluminescence and field emission properties. *J. Phys. Chem. C* **111**(6), 2470–2476 (2007)
25. Monticone, S., Tufeu, R., Kanaev, A.V.: Complex nature of the UV and visible fluorescence of colloidal ZnO nanoparticles. *J. Phys. Chem. B* **102**, 2854–2862 (1998)